be of the order of 10^3 M^{-1} at 298 K when B is 2,6-dimethylpyridine.[14] Since the hydrogen-bonding equilibrium is expected to be exceedingly rapid, these data support the interpretation presented in the previous paragraph for the rapid proton-transfer reactions.

The second-order rate constant (Table II) for the reaction of $PA\text{-}NH_2^{\bullet+}$ with TBP exceeds that for the transfer of a benzylic proton from $PA\text{-}CH_3^{\bullet+}$ to TBP by more than 10^4 even though the latter reaction is thermodynamically more favorable by a factor of 10^{14}. A similar comparison for the reactions of $PA\text{-}H^{\bullet+}$ and $PA\text{-}CH_3^{\bullet+}$ with TBP reveals that the former reacts 5 times as fast in spite of the fact that the equilibrium constant is 14 orders of magnitude less favorable. This apparent inverse dependence of kinetic on thermodynamic acidities further illustrates the complexities of cation radical deprotonation reactions. Likewise, there is no direct relationship between cation radical reduction potential and kinetic acidities in this series of reactions.

We suggest that charge distribution and the identity of the atom to which the proton is attached are important features in determining the relative kinetic acidities in this series of cation radicals. In both $PA\text{-}NH_2^{\bullet+}$ and $PA\text{-}H^{\bullet+}$ there is considerable charge on the atom to which the acidic proton is attached while this is not the case for $PA\text{-}CH_3^{\bullet+}$.

Acknowledgment. This research was supported by the National Science Foundation (CHE-8803480) and the donors of the Petroleum Research Fund, administered by the American Chemical Society. We thank Professor F. G. Bordwell for providing unpublished pK_a data.

(14) Hydrogen-bonding equilibrium constants have been determined from reversible electrode potentials in a number of cases; for example, see: Parker, V. D. *Acta Chem. Scand.* **1984**, *B38*, 125, 189. Eliason, R.; Parker, V. D. *Acta Chem. Scand.* **1984**, *B38*, 741. Svaan, M.; Parker, V. D. *Acta Chem. Scand.* **1985**, *B39*, 401. Svaan, M.; Parker, V. D. *Acta Chem. Scand.* **1986**, *B40*, 36.

Transition Structure for the Epoxidation of Alkenes with Peroxy Acids. A Theoretical Study

Robert D. Bach,* Amy L. Owensby, Carlos Gonzalez, and H. Bernard Schlegel

Department of Chemistry, Wayne State University Detroit, Michigan 48202

Joseph J. W. McDouall

Department of Chemistry, University of Manchester Manchester M139PL, U.K.

Received November 5, 1990

Despite the importance of chemical transformations involving organic peroxides, the mechanistic details of oxygen transfer remain obscure. We recently employed hydrogen peroxide as a model oxidant for ab initio studies on the oxidation of ammonia.[1] The potential energy surface for oxygen atom transfer was dominated by the 1,2-hydrogen shift in H_2O_2 forming water oxide, $H_2O^+\text{–}O^-$ (56.0 kcal/mol barrier), followed by a facile S_N2 like displacement by NH_3 on $H_2O^+\text{–}O^-$ (1.7 kcal/mol barrier) to afford $H_3NO + H_2O$. Oxidation by a peroxy acid could potentially occur by a similar pathway involving either a 1,2- or a 1,4-hydrogen shift prior to or after oxygen atom transfer. Enthalpic considerations suggest that breaking both the O–H and O–O bonds of the peracid in the transition state (TS) would be energetically unfavorable. We now report that epoxidation of ethylene by peroxyformic acid proceeds by a distinctly different mechanism than that found for hydrogen peroxide.[1]

We first examined the relative energies of the two zwitterionic species arising from 1,2- and 1,4-hydrogen shifts in peroxyformic acid (**1**). Dioxygen ylide **1a** and hydroxycarbonyl oxide **1b** are

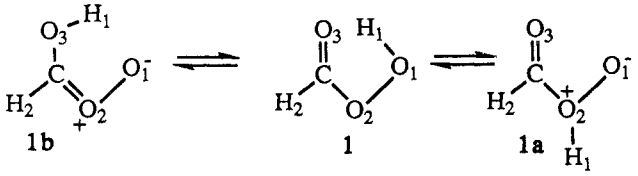

calculated to be 55.5 and 28.8 kcal/mol higher in energy than **1**, but the barrier for reversion of **1b** to **1** is only 1.7 kcal/mol (HF/6-31G*).[2] As in HOOH → H_2OO, the barrier disappears when MP4 correlation corrections are included.[3] With geometry optimization at the MP2/6-31G* level, water oxide does exist as a local minimum;[1a] by contrast, zwitterion **1b** is not a local minimum at MP2/6-31G* and optimized directly to **1**.[4] When the $O_3\text{–}H_1$ bond in **1b** was constrained (0.98 Å), it was 33.4 kcal/mol higher in energy than **1**. Although this energy difference is considerably higher than the magnitude of a typical activation barrier for epoxidation (15–18 kcal/mol),[5] we could not exclude a protonation–deprotonation sequence like that noted[1b] for H_2O_2 because the intrinsic barrier for oxygen atom transfer from the parent carbonyl oxide ($H_2C{=}O^+\text{—}O^-$) to ethylene is only 13.9 kcal/mol (MP4/6-31G*//MP2/6-31G*).

In the only previous ab initio study of alkene epoxidation, Plesnicar examined five plausible transition states and reported a barrier of 16 kcal/mol (STO-4G) for an unsymmetrical TS where peroxyformic acid was directly over one of the methylene carbons of ethylene.[6] Our search at the HF/3-21G level led to only one first-order saddle point, TS-**2**, resulting from oxygen atom transfer from hydroxycarbonyl oxide **1b**. This TS exhibits a single imaginary frequency both at HF/3-21G and at HF/6-31G*. However, the MP4/6-31G*//HF/6-31G* activation barrier of 41.4 kcal/mol was disturbingly high.[5,7] Prior experience with the calculations involving O–O bond cleavage[1] prompted a search of this potential energy surface at MP2/6-31G*. In an attempt to locate spiro TS-**2**, we constrained the $O_3\text{–}H_1$ bond distances at 0.99 and 1.09 and reoptimized the transition state in the space of the remaining parameters. These structures were 39.4 and 34.7 kcal/mol above isolated reactants, respectively. In each case release of that geometry constraint resulted in hydrogen transfer (H_1 to O_1) affording TS-**3a**. Although TS-**3a** is a second-order saddle point at HF/3-21G, a frequency calculation (HF/6-31G*) established the validity of this TS at geometries optimized at both the HF/6-31G* and MP2/6-31G* levels; the corresponding MP4 barriers of 15.7 and 16.5 kcal/mol are in excellent agreement with experiment (Figure 1).[5,8] We also find that spiro TS-**3a** is 9.2

(1) (a) Bach, R. D.; McDouall, J. J. W.; Owensby, A. L.; Schlegel, H. B. *J. Am. Chem. Soc.* **1990**, *112*, 7064, (b) 7065. (c) Bach, R. D.; Owensby, A. L.; Gonzalez, C.; Schlegel, H. B.; McDouall, J. J. W. *J. Am. Chem. Soc.*, submitted.

(2) (a) Molecular orbital calculations have been carried out using the GAUSSIAN 88 program system[2b] utilizing gradient geometry optimization.[2c] (b) M. J. Frisch, M. Head-Gordon, H. B. Schlegel, K. Raghavachari, J. S. Binkley, C. Gonzalez, D. J. DeFrees, D. J. Fox, R. A. Whiteside, R. Seeger, C. F. Melius, J. Baker, R. L. Martin, L. R. Kahn, J. J. P. Stewart, E. M. Fluder, S. Topiol, J. A. Pople, Gaussian, Inc., Pittsburgh, PA, 1988. (c) Schlegel, H. B. *J. Comput. Chem.* **1982**, *3*, 214. (d) Gonzalez, C.; Schlegel, H. B. *J. Phys. Chem.* **1990**, *94*, 5523. Step size of 0.2 $amu^{1/2}$-bohr used.

(3) DeFrees, D. J.; Raghavachari, K.; Schlegel, H. B.; Pople, J. A. *J. Am. Chem. Soc.* **1982**, *104*, 5576.

(4) (a) The MP2/6-31G* geometry of peroxyformic acid is in excellent agreement with microwave spectral data (in parentheses)[4b] where $O_1\text{–}O_2$ = 1.46 Å (1.45), $C\text{–}O_2$ = 1.35 Å (1.34), $C\text{–}O_3$ = 1.22 Å (1.20), $O_1\text{–}H_1$ = 0.99 Å (1.02), and $\angle O_2O_1H_1$ = 100.3° (99.2). (b) Oldani, M.; Ha, T.-K.; Bauder, A. *J. Am. Chem. Soc.* **1983**, *105*, 360.

(5) Dryuk, V. G. *Tetrahedron* **1976**, *32*, 2855.

(6) The TS geometry, optimized with the STO-2G basis prior to the availability of gradient optimization, was a higher order saddle point that differed significantly from the first-order TS that we now report. Plesnicar, B.; Tasevski, M.; Azman, A. *J. Am. Chem. Soc.* **1978**, *100*, 743.

(7) HF/6-31G* calculations incorrectly predict TS-**2** to be 12.1 kcal/mol more stable than TS-**3a**. The major effect of electron correlation is the improvement of the description of the O–O bond in TS-**3a**.

(8) Although the HF wavefunction to TS-**3a** is UHF unstable, there was no significant change in the barrier calculated at the UMP4 level with spin projection (18.9 kcal/mol, PMP4(SDTQ)/6-31G*//RMP2/6-31G*) or at the RQCISD(T)/6-31G*//MP2/6-31G* level (19.7 kcal/mol).

0002-7863/91/1513-2338$02.50/0 © 1991 American Chemical Society

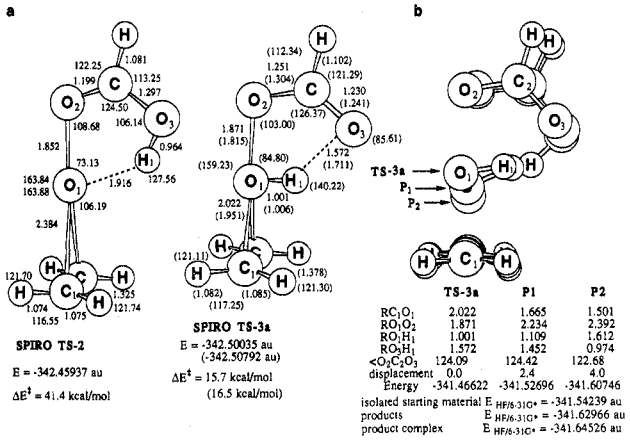

Figure 1. (a) Comparison between the transition states of peroxyformic acid zwitterion + ethylene (**TS-2**) and peroxyformic acid + ethylene (**TS-3a**) (optimized structures at the HF/6-31G* level, MP2/6-31G* geometry in parentheses; MP4SDTQ/6-31G*//HF/6-31G* energies in au, MP4SDTQ/6-31G*//MP2/6-31G* values in parentheses). (b) **TS-3a** and two intermediate points (P_1 and P_2) along the path toward products, ethylene oxide and formic acid (IRC at HF/6-31G*, displacement in amu$^{1/2}$·bohr).

kcal/mol more stable than a planar **TS-3b** and 8.4 kcal/mol lower in energy than an unsymmetrical structure[6] (both are second-order saddle points, MP4SDTQ/6-31G*//HF/6-31G*). As long as H_1 is strongly bound to its "electrophilic" oxygen, then the two lone pairs of electrons on that oxygen will differ in energy, potentially displaying a preference for orientation of attack on the alkene, which obviously arises from an electronic effect since steric interactions involved in this system are minimal. However, the oxenoid oxygen in **TS-2** has essentially spherical electron density, and no such stereoelectronic effects should be anticipated.

Figure 1b provides several "snapshots" along the intrinsic reaction path[2d] from **TS-3a** toward products. Rehybridization at ethylene is minimal at the TS while the O_2–C_2 bond shortens toward a carbonyl bond distance, the C_2–O_3 lengthens as the hydrogen is transferred, and the C_1–O_1 bonds of the epoxide develop. The relatively low activation barrier when compared to H_2O_2 is a reflection of the more idealized molecular architecture of the peracid functional group that has a developing carboxylate anion ideally poised to accept the migrating hydrogen *after the barrier is crossed* and to stabilize by resonance the charge on the leaving formate fragment as depicted in Figure 1b by the alternating C–O bond distances. This transition structure provides a theoretical corroboration of the generally accepted "butterfly" mechanism first disclosed by Bartlett[9] at this institution in 1950 and is consistent with a relatively low deuterium isotope effect, $k_H/k_D = 1.17$ (RO_1–$H_1 = 1.001$ Å).[10] This TS is also consistent with our earlier suggestion of an S_N2 attack by the alkene π-bond on the σ and σ^* orbitals of the O–O bond[11a,b] in consonance with the four-electron, three-MO frontier MO model.[11c] We attribute the electrophilicity of a peracid to its relatively weak O–O bond that can provide an empty (electrophilic) σ^* orbital early along the reaction coordinate that can mix with the nucleophilic π-bond.

Acknowledgment. This work was supported in part by a grant from the National Science Foundation (CHE-87-11901), the National Institutes of Health (CA 47348-02), and Ford Motor Company. We are very thankful to the Pittsburgh Supercomputing Center, the Ford Motor Company, and the Computing Center at Wayne State University for generous amounts of computing time.

(9) Bartlett, P. D. *Rec. Chem. Prog.* **1950**, *11*, 47.
(10) Hanzlik, R. P.; Shearer, G. O. *J. Am. Chem. Soc.* **1975**, *97*, 5231.
(11) (a) Bach, R. D.; Willis, C. L.; Domadala, J. M. In *Applications of Molecular Orbital Theory in Organic Chemistry*; Csimadia, I. G., Ed.; Elsevier: Amsterdam, 1977; pp 221-229. (b) Lang, T. J.; Wolber G. J.; Bach, R. D. *J. Am. Chem. Soc.* **1981**, *103*, 3275. (c) Bach, R. D.; Wolber, G. J. *J. Am. Chem. Soc.* **1984**, *106*, 1410.

FK506 and Rapamycin Binding to FKBP: Common Elements in Immunophilin–Ligand Complexation

Thomas J. Wandless, Stephen W. Michnick, Michael K. Rosen, Martin Karplus,* and Stuart L. Schreiber*

Department of Chemistry, Harvard University Cambridge, Massachusetts 02138

Received December 4, 1990

Complexes of immunophilins and their ligands have been shown to inhibit signal transduction pathways that result in exocytosis and transcription.[1] For example, recent studies demonstrate that FK506[2,3] and rapamycin[4] bind to the same immunophilin, FKBP, and suggest that distinct signaling pathways are inhibited by complexes formed between an immunophilin (possibly FKBP) and either FK506 or rapamycin.[5,6]

Investigations of human recombinant FKBP,[7,8] isotopically labeled FK506,[9,10] and the nonnatural FKBP ligand 506BD led to the proposal that FK506 and rapamycin bind FKBP with similar structural elements, which include the pipecolinyl ring, and in a similar orientation.[6] The common immunophilin binding element of these agents, which is responsible for rotamase inhibition, is fused to distinct effector elements that apparently determine which signaling pathway will be inhibited. We have prepared several selectively deuterated variants of FKBP and examined the resultant FKBP/FK506 complexes by 1D and 2D NMR spectroscopy. The results show that the common pipecolinyl moiety of FK506 and rapamycin is involved in binding to FKBP and is likely to be oriented in a similar manner in the two ligand–receptor complexes.

Comparison of the ^{1}H NMR spectra of free FKBP, the FKBP/FK506 complex, and the FKBP/rapamycin complex reveals several strongly upfield shifted resonances that are similar in the spectra of the two complexes (Figure 1). To minimize signal overlap between drug and protein, several selectively deuterated FKBPs were overexpressed in *Escherichia coli*.[7] The variant discussed below contained only the four protonated amino acid types: proline, tryptophan, tyrosine, and valine.[11,12] 2D DQF-COSY spectra of FKBP/FK506 were used to identify a single spin system consisting of three methylene groups (δ 0.22 to −1.91) within these upfield resonances (Figure 2A). One of these resonances shows *J*-coupling as well as strong NOESY cross peaks to a downfield methylene group (δ 2.47, 3.17). A methylene group at the other end of the spin system shows strong NOEs from both hydrogens to a resonance at δ 4.52. There is no coupling in the DQF-COSY spectra between these resonances. Thus, six resonances in the upfield region belong to a spin system consisting

(1) Schreiber, S. L. *Science* **1991**, *251*, 283-287.
(2) Harding, M. W.; Galat, A.; Uehling, D. E.; Schreiber, S. L. *Nature* **1989**, *341*, 758-760.
(3) Siekierka, J. J.; Hung, S. H. Y.; Poe, M.; Lin, C. S.; Sigal, N. H. *Nature* **1989**, *341*, 755-759.
(4) Fretz, H.; Albers, M. W.; Galat, A.; Standaert, R. F.; Lane, W. S.; Burakoff, S. J.; Bierer, B. E.; Schreiber, S. L. *J. Am. Chem. Soc.* **1991**, *113*, 1409-1411.
(5) Bierer, B. E.; Matila, P. S.; Standaert, R. F.; Herzenberg, L. A.; Burakoff, S. J.; Crabtree, G.; Schreiber, S. L. *Proc. Natl. Acad. Sci. U.S.A.* **1990**, *87*, 9231-9235.
(6) Bierer, B. E.; Somers, P. K.; Wandless, T. J.; Burakoff, S. J.; Schreiber, S. L. *Science* **1990**, *250*, 556-559.
(7) Standaert, R. F.; Galat, A.; Verdine, G. L.; Schreiber, S. L. *Nature* **1990**, *346*, 671-674.
(8) Albers, M. W.; Walsh, C. T.; Schreiber, S. L. *J. Org. Chem.* **1990**, *55*, 4984-4986.
(9) Nakatsuka, M.; Ragan, J. A.; Sammakia, T.; Smith, D. B.; Uehling, D. E.; Schreiber, S. L. *J. Am. Chem. Soc.* **1990**, *112*, 5583-5601.
(10) Rosen, M. K.; Standaert, R. F.; Galat, A.; Schreiber, S. L. *Science* **1990**, *248*, 863-866.
(11) Two other partially deuterated FKBPs were prepared[7] containing protonated amino acids only at the following positions: Phe, Leu, and Tyr by the method in ref 12a and a variant containing Pro, Val, Trp, Tyr, and Ser by the method in ref 12b.
(12) The deuterated proteins were prepared by two methods: (a) Arrowsmith, C. H.; Pachter, R.; Altman, R. B.; Iyer, S. B.; Jardetzky, O. *Biochemistry* **1990**, *29*, 6332-6341. (b) LeMaster, D. M. *Q. Rev. Biophys.* **1990**, *23*, 133-174.

0002-7863/91/1513-2339$02.50/0 © 1991 American Chemical Society